An Hybridization Method for Absolute Radiometric Calibration Using AI Techniques

[1] Priti Tyagi, [2] Udhav Bhosle

[1] PVPP College of Engineering, Mumbai University

[2] Rajiv Gandhi Institute of Technology, Mumbai University

tpriti15@rediffmail.com

Abstract

In environmental monitoring and modeling, a key role is played by satellite image analysis throughout the precedent few decades. The capability of several types of change detection analysis is achieved by regular observation on a specified region over time. These can be complicated as variations in sensor calibration, changes in illumination and observation angles, and differences in atmospheric effects cause radiometric inconsistency. Generation of high quality science data and thereby higher level downstream items by surpassing these impediments necessitates radiometric characterization and calibration. The proposed hybridization method realizes registration of the satellite images for prediction purpose by carrying out the absolute radiometric calibration task. ANN and evolutionary GA are used in our proposed method to accomplish this task.

Keywords

Artificial Neural Network; Genetic Algorithm; Absolute Radiometric Calibration; Image Registration

Introduction

Image registration is the method to convert diverse groups of data into single coordinate system. Data may be in the form of multiple photographs, data from diverse sensors, diverse times, or diverse viewpoints. Radiometric calibration is used in the registration process of remote sensing images. Pre-launch is conducted by the calibration study to define the requirements and it recommends the use of post-launch in the procedure [13]. Calibration work is uniformly absolute and relative. Here, the term absolute calibration signifies techniques that allow the digital data to be converted to radiance. The detector's responses are normalized to an average or reference response, by categorizing the multiplicative (gain) and additive (bias) factors using relative methods like histogram equalization [14]. Radiometric calibration of a remote sensing system is used to solve the problem of accomplishing radiometric fidelity of an imaging system (Edirisinghe *et al,* 2001). The radiometric calibration of these systems more importantly permits use of the complete Land sat data set to be used in a quantitative sense applications like land use and land-cover change in addition to facilitating operation characterization of the sensors (Thome, 2001) (Thorne *et al*, 1997) (Kurtis & Thome, 2002).

Characterization of the instrument operation is facilitated by radiometric calibration of the sensors, but more significantly, use of the entire Land sat data archive is permitted in a quantitative sense by the calibration (Chander *et al,* 2004) (Chander, 2010). Data is located in a radiometric scale by absolute radiometric calibration and makes it compatible and comparable with the data acquired from diverse sensors. Determining the SAR system against standard targets with eminent radar cross section is the objective of Absolute Radiometric Calibration (Schwerdt *et al,* 2010). A precise measurement of the apparent target reflectance or radiance is permitted by radiometrically calibrated remote imaging systems at the sensor's operational altitude (Edirisinghe *et al,* 2001). Techniques based on reflectance, irradiance and radiance have been created for absolute radiometric calibration (Gurol *et al,* 2008). Method based on conventional reflectance is the most widely used method of indirect calibration (Emily 2000) (Honjo, 2001). The surface of a test site and the atmosphere over that test site are characterized with the reflectance-based method using ground-based measurements (Thome, 2008) (Kurt Thome, 2010) .

Utilization of reflectance to compare images from various sensors has two advantages. Firstly, the possibility to eliminate time difference between data acquisitions results in the occurrence of the cosine effect of diverse solar zenith angles. Secondly, spectral band differences causing diverse values of the exo-atmospheric solar irradiances are compensated by it (Chander *et al*, 2004) (Teillet *et al*, 2001) (Chander *et al*,

2008). Radiance based techniques making a comparison among all the digital numbers present in the stellar image are the absolute in-band spectral radiance of several radiometrically characterized images to perform absolute calibration of the IKONOS satellite's payload sensors (Howard & Bowen, 2002). A well-calibrated radiometer is used by radiance-based sensor methods to make measurement of the upwelling radiance from the test site from an aircraft. Later, the radiances at the sensor are perceived by further restriction on the radiative transfer code computations using these radiances (Thorne *et al*, 1997) (Teillet, 2001). The field radiance measurements are reliable and partitioned to the visualized irradiance measurements to evaluate the reflectance in these wavelengths (Vries *et al*, 2004) (Vriesa *et al*, 2007).

The proposed hybrid absolute radiometric calibration technique is carried out in three phases. In the first phase, the calibration coefficients are predicted by ANN using the historical lifetime data. In the second phase, the calibration coefficients are interpreted by the Evolutionary GA algorithm. Finally in the third phase the calibrated image of the sensor image is obtained from registration using the above obtained calibration coefficient. The structure of the paper is organized as follows: A brief review of the researches related to the absolute calibration coefficient is given in Section 2. The proposed hybridization calibration technique is given in section 3. The experimental results of the proposed approach are presented in Section 4. Finally, the conclusions are given in Section 5.

Related Works

Xulin Guo *et al.* (2008) have identified that inconsistent results could be obtained from the same image in different formats when a System Pour I' Observation de la Terre 4 high resolution visual and infrared 2 (HRVIR2) image is preprocessed. The source of error has been examined by means of the two different SPOT image formats, Centre d' Archivage et de Pretraitement (CAP) and digital image map (DIMAP). The CAP and DIMAP format have obtained different radiance values of the near-infrared (NIR) and red bands when the digital numbers (DNs) were translated. They have identified that a mismatch between the band sequences and absolute radiometric calibration gains has been the cause for this inconsistency. Therefore, it was confirmed that the band sequences has been always necessary prior to the application of any calibration coefficients in the course of the use of SPOT with level 1A (L1A) products.

Jinjun Tong *et al.* (2009) have discussed that an Automated Hydro Meteorological Buoy (AHMB) system has been used to quantify the surface water temperatures of QHL and the data inputted into the atmospheric transfer model MODTRAN3.7 for thermal infrared (TIR) channels of FY-2C has been reviewed by the atmospheric profiles over QHL from the National Centers for Environmental Prediction (NCEP) for evaluation of the entrance pupil radiance and brightness temperatures. Then, the equivalent blackbody (EBB) temperatures TEBB have been calculated through an absolute radiometric calibration coefficient of FY-2C by comparing the entrance pupil radiance and brightness temperatures with the equivalent DNs. In addition, they have remotely calculated the Temperatures of Onboard Blackbody (OBB) TOBB, primary, secondary, refraction, and calibration mirrors on the multi-channel scanning radiometer (MSR) of FY-2C. Linear correlation between TEBB 2 TOBB and temperatures of diverse mirrors has been used as the basis to develop the transform equations from TOBB to TEBB. Finally, the uncertainty with which the onboard real-time absolute radiometric calibration for TIR channels of geostationary meteorological satellite FY-2C implemented for TIR 1 and TIR 2 has been around 1.5 and 2.1 K respectively.

Andrea Baraldi (2009) has considered the necessary but not sufficient condition to implement operational automatic RS-IUSs, namely radiometric calibration of RS images, unlike other existing literature. This necessity has been a supplement to the conventional view that calibration and validation (Cal/Val)-related activities are highly important to realize harmonization and interoperability of multi-source EO data and derived information products have been produced at all scales as perceived by (i) the European Union (EU) led Global Monitoring for the Environment and Security (GMES) project and (ii) the Group on Earth Observations (GEO) that has been developed by the program called Global Earth Observation System of Systems (GEOSS) of which the Committee of Earth Observations (CEOS) has provided a Quality Assurance Framework for Earth Observation (QA4EO) data as its space arm. Supporting the RS community to perform additional analysis on the calibration quality and ambiguity of the Satellite Pour l'Observation de la Terre (SPOT) and Indian Remote sensing Satellite (IRS) imaging sensor

series, for which the zero-value offset parameters have appeared controversial on the basis of experimental data, has been their second objective. Thirdly, a quantitative estimation of the spectral information loss with regard to the current SPOT-4/-5 optical sensors may distress the future planned European EO satellites like Pleiades-1/-2 and the follow-on missions Astrium SPOT-6/-7. Lastly, their work has revealed that the compulsory radiometric calibration preprocessing stage has been apparently ignored miserably or taken too lightly in numerous recent or current scientific applications of EO images obtained across time, space, and sensors by the EU space agencies and research institutions that have been participants in CEOS for over twenty years and they should be keen on converting the new QA4EO scheme into RS common practice.

Tongjiang Wang *et al.* (2009) have proposed a method that uses in which a combination of solar LW spectra and density- and temperature- insensitive line intensity ratios for to obtaining short wavelength (SW) channel is utilized. An intensity calibration, updated for the CDS NIS-1 waveband performed in the initial phase using the coordinated, co spatial EUNIS and SOHO/CDS spectra has demonstrated that its efficiency is reduced by a factor about 1.7 in comparison with the formerly implemented calibration. Then, the identification of the exact emission lines intensity inside the EUNIS SW band pass from those of co spatial CDS/NIS-1 spectra has been permitted by the theoretical insensitive line ratios acquired from CHIANTI subsequent to the EUNIS LW calibration adjustment. A valuable response curve for the EUNIS-06 SW channel that matches properly to a relative calibration dependent on uniting measurements of distinct optical components has been provided by a total of 12 ratios n derived from intensities of 5 CDS and 12 SW emission lines from Fe x–Fe xiii. They have estimated the accuracy of EUNIS-06 SW absolute calibration as ±20%by considering all possible sources of error.

Jinjun Tong *et al.* (2010) have analyzed the possibility of an alternative method for the Chinese meteorological satellites Feng Yun – 2B(FY-2B) and Feng Yun - 2C(FY-2C) for exact in-flight radiometric calibration of the thermal infrared channels. Radiosonde atmospheric profiles and the water surface brightness from TIR radiometers (CE312) have been substituted with those from the National Centers for Environmental Prediction (NCEP) reanalysis and an automated hydro meteorological buoy (AHMB) system respectively over the Qinghai Lake (QHL) of China by means of the proposed alternative method. Then, the calibration coefficients and their uncertainty for the TIR channels of FY-2B and FY-2C have been computed utilizing these data. 14 atmospheric profiles as evaluated by radiosonde over QHL in August 2003 and the equivalent NCEP reanalysis data have been used to calculate the At-Sensor Radiance (ASR) and At-Sensor Brightness Temperature (ASBT) of the TIR channels of FY-2B and FY-2C respectively. As well they have conducted sensitivity tests on the ASR and ASBT of the TIR channels of FY-2B and FY-2C for diverse atmospheric profiles having diverse relative humidity and air temperatures. The gain difference has been less than 0.005 mW m(–2) sr(-1) cm(-1) DN-1 in between the standard and alternative methods. The ASR and ASBT have been proved to be more sensitive to relative humidity than that to temperature in the atmospheric profile by sensitivity tests, which has proved by experimental results that the uncertainty of the proposed alternative method around 1.5 K for the TIR channels of FY-2B and FY-2C is possible for the TIR channels of diverse remote sensors. Potential for more frequent, dependable and economical calibrations of the TIR sensors in operational conditions has been one of the major advantages of their proposed method.

Absolute Radiometric Calibration Finding by Means of ANN and GA

The ability to detect and quantify the changes in the earth's environment depends on the sensors that can provide calibrated (known accuracy and precision) and consistent measurements of the earth surface features in the course of time. The correct interpretation of the scientific information from a global, long-term series of remote-sensing products requires the ability to discriminate between product artifacts and changes in the earth process monitored (Borak *et al*, 2002). Radiometric characterization and calibration is a pre requisite to create high quality science data, and consequently higher level down-stream products. The ultimate goal of the calibration teams under process is to characterize the instrument and provide accurate radiometric calibration for any point in its lifetime. The proposed hybrid calibration technique involving the Artificial Neural Network and genetic algorithm deals with the calibration procedure by using the lifetime vicarious gain coefficients and offset value. Subsequently, the related upcoming gain and offset values are calibrated and thereby the future

image related to the reference image is predicted. Let ' $R1$ ' and ' $R2$ ' be the reference images and $D = \{D_{ij} \mid i = 1,\cdots,M\,;\, j = 1,\cdots,N\}$ be the life time vicarious gain coefficients in digital numbers per unit radiances watts per square meter per steradian per micron for the days and $D1 = \{D1_{ij} \mid i = 1,\cdots,M\,;\, j = 1,\cdots,N\}$ be the offset coefficients where ' M ' is the no. of bands and ' N ' be the no. of days from the launch of the satellite. The proposed calibration technique is carried out in three phases namely (i) calibration coefficients prediction using historical life time coefficients, (ii) Blind-trial reference based calibration coefficients interpretation and (iii) Image registration.

Calibration Coefficients Prediction Using Life Time Coefficients

In this phase the calibration coefficients are predicted by means of an ANN using the lifetime coefficients value and two ANN are trained by the life time gain and offset values for every band separately. In the testing section the gain and offset values for the future days are predicted using the trained ANN, first of which is trained using historical lifetime coefficient ' D ' and the other is trained using the coefficient ' $D1$ '. Fig.1 shows the sample two inputs and single output neural network sample structure.

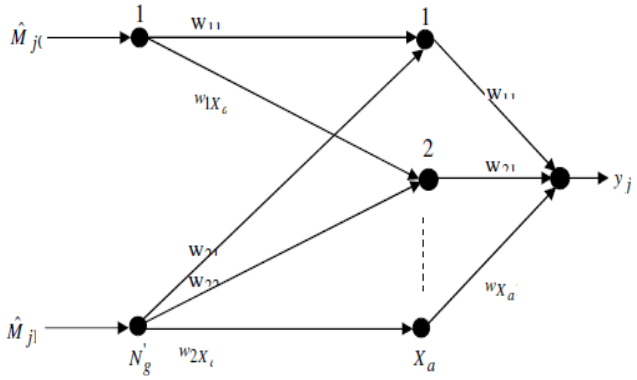

FIG. 1 TWO INPUTS-1 OUTPUT NEURAL NETWORK STRUCTURE

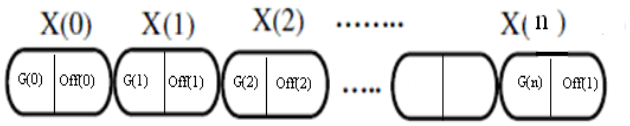

FIG.2. STRUCTURE OF THE POPULATION

N input is represented as $\hat{M}_{jo}$ and $\hat{M}_{j1}$ exists in the artificial neuron presented in Fig.2. A weight represented as $w_{11}, w_{12}, \cdots, w_{1N}$ respectively is assigned to each line that connects these inputs to the neuron. λ Normally represents the threshold in artificial neuron and the following formula is used to determine the activation.

$$y_j = \alpha + \sum_{k=0}^{N_g'-1} w_{jk}\,\hat{M}_{jk} \quad 0 \le j \le N_s' - 1 \qquad (1)$$

$$g(y) = \frac{1}{1+e^{-y}} \qquad (2)$$

$$g(y) = y \qquad (3)$$

The basis function (specified only for input layer) is given in Eq. (1) and the sigmoid and identity activation function, selected for hidden and output layer are given by Eq. (2) and Eq. (5) respectively. In Eq. (1), $\hat{M}$, w_{jk} and α are the days from the launch, weight of the neurons and bias respectively.

All the remaining layers (hidden and output layer) normally use the basis function given in Eq. (1) (but with the number of hidden and output neurons respectively). The output from N_p ANNs is determined by giving $\hat{M}$ as input to all those layers. A single value ' y_i ' is obtained from this method by combining both the weights. Likewise the second ANN is trained using the historical lifetime offset values of each band and the output ' z_i ' is obtained for each band. By using the trained ANN the calibration coefficients gain ' $G1$ ' and offset ' $Of1$ ' values are predicted for the future day 'DA'.

Blind-Trial, Reference Model Based Calibration Coefficients Interpretation

In this phase the calibration coefficients gain and offset are interpreted using the Genetic algorithm by means of the two reference images $R1$ and $R2$. The population with 'n' chromosomes is generated, each of which consists of blindly fixed gain and offset values. In order to find the optimized calibration coefficients, blind-trial method is used and the calibration coefficients are blindly fixed for each chromosome in the initial iteration

Fig. 2 illustrates the structure of the chromosome. $X_0, X_1 \cdots X_{|n|}$ are the chromosomes of the population, $G(0), G(1) \cdots G(n)$ are the gain calibration efficiency and $Off\,(0), Off\,(1) \ldots Off\,(n)$ are the offset of the chromosome which is blindly fixed. To find the fitness of the

chromosome, the reference images '$R1$' and '$R2$' are used and the following function is used to find the fitness of the chromosome.

$$\frac{1}{l*m}\sum_{i=1;\,j=1}^{l;m}\sqrt{(R1_{ij})^2-(R2_{ij}*G(k)+Off(k))^2}\;;1<k<n$$

Where l is the row size of the reference images, m is the column size of the reference images and n is the no. of chromosomes.

Owing to the fact that mutation helps to prevent the population from stagnating at any local optima, it is considered as an important part of the genetic search. Mutation operator is executed in accordance with a user-definable mutation probability during the evolution. According to the fitness function, the first 'r' chromosomes are chosen and then mutated by random values to get r' chromosomes so that the new population contains $r+r'$ chromosomes. The above processes of fitness finding and mutation operation are repeated for 'NN' times and the first chromosome in the final iteration is the optimum one. Subsequently, the gain and offset values are optimized. The optimized calibration coefficients Gain '$G2$' and offset '$Of2$' are interpreted by the blind-trial method using the reference images 'R1' and 'R2'.

Image Registration

In this phase the sensor image I is registered by using the radiometric calibration coefficients '$G1$', '$Of1$' and '$G2$', '$Of2$' which are predicted and interpreted respectively. The registered image $\hat{I}$ of the orbital sensor image I is accomplished with the aid of the two images '$\hat{I}1$' and '$\hat{I}2$' where $\hat{I}=\hat{I}1+\hat{I}2$

$$\hat{I}1=I1_{ij}*\frac{128}{I1_{\max}-I1_{\min}}\;;\;\hat{I}2=I2_{ij}*\frac{128}{I2_{\max}-I2_{\min}}$$

$$I1_{ij}=I_{ij}*G1+Of1 \quad \text{And} \quad I2_{ij}=I_{ij}*G2+Of2\,;$$

$1<i\le l$; $1<j\le m$; l and m are the row and column size of the image. $I1_{\max}$, $I1_{\min}$ and $I2_{\max}$, $I2_{\min}$ are maximum and minimum pixel values of the $I1$ and $I2$ respectively. By using the calibration coefficients $G1$, $G2$, $Of1$ and $Of2$, $I1$ and $I2$ are interpreted. Subsequently, the interpreted image is normalized and $\hat{I}1$ and $\hat{I}2$ are obtained. Finally the image registration of the orbital sensor image is obtained by using the calibration coefficients.

Experimental Results

The proposed radiometric calibration has been implemented in the working platform of MATLAB (version 7.10) and its performance was evaluated using the sensor image database. The proposed technology primarily deals with the development of procedure to find the calibration coefficient values thereby the forecasting registered image of the satellite image. For experimentation, historical life time, gain values and the offset values of the R, G, B band, obtained from a satellite sensor are used. The ANN1 is trained using the obtained gain of the red band value and the ANN2 is trained using the offset value. Subsequently, gain '$G1$' and offset '$Of1$' are obtained for the future day 'DA'.

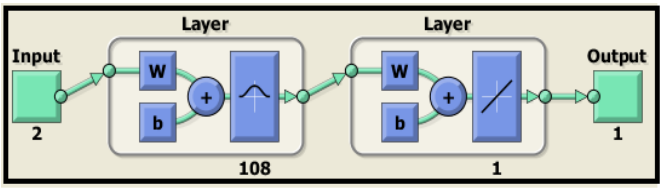

FIG. 3 STRUCTURE OF THE ANN1

Fig. 3 illustrates the structure of the ANN1 used to train and test the gain values.

And Fig. 4 illustrates the structure of the ANN2 used to train and test the offset values. The band no as well as the no of days from the launch is given as input to the ANN.

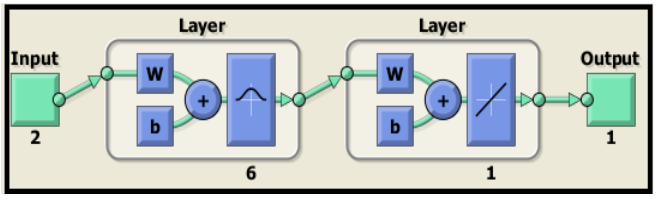

FIG. 4 STRUCTURE OF THE ANN2

Based on evolutionary GA which uses the blind trial method for the parameter, the values of fitness function, gain $G2$ and offset $Of2$ are interpreted. The obtained calibration coefficients values are employed to obtain the registered sensor image for the specified query image.

Fig. 5 illustrates the input satellite image with the PSNR value +27.00 dB. By means of the predicted calibration coefficients '$G1$' and '$Of1$', the Registered Image-1 obtained is shown in fig 6 and Registeredimage-2 obtained by the interpreted

calibration coefficients' $G2'$ and '$Of2'$ is shown in fig 7. The Fig 8(a), (b), (c), (d) show the forecast, registered image of the input image obtained using the reference image-1 and reference image-2 in the iteration no 10,100,200,300,400 and 500 respectively. Though the difference of the forecasted images and the input image is not obvious, the registered image achieves better PSNR value compared to the original input image. The PSNR improvement may be insignificant, however, the prediction model which is not in the literature, is able to register an image in any of the upcoming days.

FIG. 5 INPUT SATELLITE IMAGE

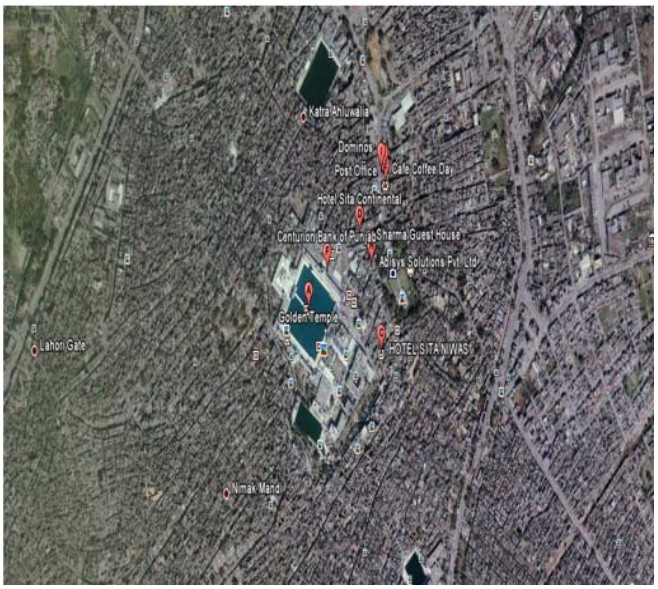

FIG. 6 THE REGISTERED IMAGE-1

FIG. 7 THE REGISTERED IMAGE-2

(a)

(b)

(c)

(d)

(e)

FIG. 8 PREDICTED REGISTERED IMAGE

Table-1 illustrates the PSNR values of the forecasted images.

TABLE 1 PSNR VALUES

Iteration No	PSNR Value
10	+ 27.00 dB
100	+ 27.01 dB
200	+ 27.02 dB
300	+ 27.02 dB
400	+ 27.06 dB

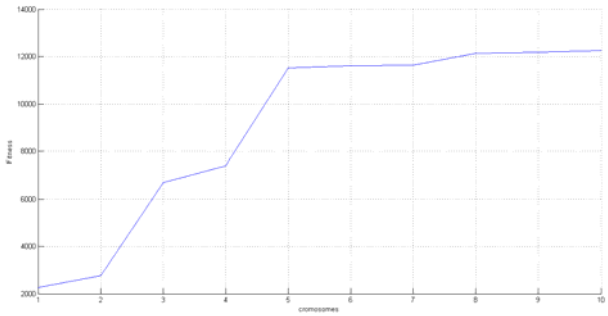

FIG. 9 CONVERGENCE GRAPH OF THE FITNESS

The above fig 9 shows convergence graph of the fitness of the chromosome in the evolutionary GA.

Conclusion

The primary intent of our research work is to solve the computational complexity and inaccurate radiometric coefficients calculation problem. The proposed approach, an effective hybridization technique developed by blending two ANN and evolutionary GA, has been implemented in the working platform of MATLAB 7.10 and its performance was evaluated. The obtained experimental results show that the proposed hybridization technique is more effective than existing methods in the reduction of hardware and computational complexities.

References

Baraldi, A. 2009, "Impact of Radiometric Calibration and Specifications of Spaceborne Optical Imaging Sensors on the Development of Operational Automatic Remote Sensing Image Understanding Systems", IEEE Journal of Selected Topics in Applied Earth Observations and Remote Sensing, Vol. 2, No. 2, pp. 104-134.

Bowen, H.S. 2002, "Absolute Radiometric Calibration of the Ikonos Sensor Using Radiometrically Characterized Stellar Sources," In Proceedings of Pecora 15/Land Satellite Information IV Conference, ISPRS Commission I

Mid-term Symposium/FIEOS (Future Intelligent Earth Observing Satellites), Denver, CO.

Chander, Coan & Scaramuzza. 2008, "Evaluation and Comparison of the IRS-P6 and the Landsat Sensors", IEEE Transactions on Geoscience and Remote Sensing, Vol. 46, No. 1, pp. 209-221.

Chander, G., Helder, D.L., Markham, B.L., Dewald., Kaita, J.D., Thome, K.J., Micijevic, E., & Ruggles, T.A., 2004, "Landsat-5 TM Reflective-Band Absolute Radiometric Calibration", IEEE Transactions on Geoscience and Remote sensing, Vol. 42, No. 12, pp. 2747-2759

Chander, Haque, Micijevic & Barsi, 2010, "A Procedure for Radiometric Recalibration of Landsat 5 TM Reflective-Band Data", IEEE Transactions on Geoscience and Remote sensing Vol. 48, No. 1, pp. 556-574.

Edirisinghe, Chapman & Louis. 2001, "A simplified method for retrieval of ground level reflectance of targets from airborne video imagery", International Journal of Remote Sensing, Vol. 22, No. 6, pp. 1127- 1141.

Edirisinghe, Louis. & Chapman. 2001, "Radiometric corrections for multispectral airborne video imagery", International Journal of Remote Sensing, Vol. 67, No. 8, pp. 915-924.

Emily, E., Whittingtona, Kutis, J., Thome, Barnes, R., A. & Canhama, K., A. 2000, "Radiometric calibration of the Sea-viewing Wide Field of View Sensor using ground-reference techniques", In Proceedings of SPIE, Vol. 4135, pp. 294-301, San Diego, CA, USA,

Guo, X. & He, Y. 2008. "Mismatch of band sequences between an image and header file:a potential error in SPOT L1A products", Canadian Journal of Remote Sensing, Vol. 34, No. 1, pp. 1-4.

Gurol, Ozen, Leloglu & Tunali. 2001, "Tuz Gölü: New Absolute Radiometric Calibration Test Site", In Proceedings of the International Archives of the Photogrammetry, Remote Sensing and Spatial Information Sciences Congress, Vol. 37, pp. 35-40, Beijing

Honjo. 2011, "A reflectance based vicarious calibration with on-site instruments monitoring", Journal of Advances in Space Research, Vol. 28, No. 1, pp. 11-20.

Jones, L., Park, J.D., Soisuvarn, S., Hong, L., Gaiser, P.W. & Germain, K.M. 2006, "Deep-Space Calibration of the WindSat Radiometer", IEEE Transactions on Geoscience and Remote Sensing, Vol. 44, No. 3, pp. 476-495.

Roy, D., Borak, J., Devadiga, S., Wolfe, R., Zheng, M., & Descloitres, J. 2002. "The MODIS land product quality assessment approach". Remote Sensing of Environment, Vol. 83, No. 62–76.

Schwerdt, Bautigam, Bachmann, Schrank, D.D. & Hueso, J., Gonzalez. 2010, "Final Results of the Efficient TerraSAR-X Calibration Method", IEEE Transactions on Geoscience and Remote Sensing, Vol. 48, No. 2, pp. 677-689.

Teillet, Fedosejevs, Gauthier, O'Neill, Thome, Biggar, Ripley & Meygret. 2001, "A generalized approach to the vicarious calibration of multiple Earth observation sensors using hyperspectral data", Journal of Remote Sensing of Environment, Vol. 77, No. 3, pp. 304-327.

Teillet, Markhamb, B., Irish, Fedosejevs. & Storey. 2001, "Radiometric cross-calibration of the Landsat-7 ETM+ and Landsat-5 TM sensors based on tandem data sets", Journal of Remote Sensing of Environment, Vol. 78, pp. 39-54.

Thome, Corkel, M. & Czapla-Myers. 2008, "Inflight Intersensor Radiometric Calibration Using the Reflectance-based Method for Landsat-Type Sensors", The 17th William T. Pecora Memorial Remote Sensing Symposium.

Thome, K. 2010, "Imaging and Field Spectrometer Data's Role in Calibrating Climate-quality Sensors", Art, Science and Applications of Reflectance Spectroscopy Symposium, pp. 1-8, Boulder, Colorado.

Thome, K.J. 2002, "Ground-look radiometric calibration approaches for remote sensing imagers in the solar reflective", In Proceedings of International Society for Photogrammetry and Remote Sensing, Denver, Colorado.

Thome. 2001, "Absolute radiometric calibration of Landsat 7 ETM+ using the reflectance-based method", Journal of Remote Sensing of Environment, Vol. 78, No. 1,2, pp. 27-38.

Thorne, Markharn, Barker, Slater & Biggar, 1997 "Radiometric Calibration of Landsat", Journal of Photogrammetric Engineering & Remote Sensing, Vol. 63, No. 7, pp. 853-858.

Tong, J., Dery, Chen, Y., Hu, B., 2010. "An alternative method for in-flight absolute radiometric calibration of

thermal infrared channels of Chinese geostationary meteorological satellites", International Journal of Remote Sensing, Vol. 31, No. 3, 10, pp. 791–803.

Tong, j., Dery, SJ., Hu, B., Chen, Y. & Yang, C. & Rong, Z. 2009, "Onboard Real-Time Absolute Radiometric Calibration for Thermal Infrared Channels of Chinese Geostationary Meteorological Satellites", Journal of Atmospheric and Oceanic Technology, Vol. 26, No. 2, pp. 281-289.

Vries, C. D., Danaher T. and Scarth, P. 2004, "Calibration of Multiple Landsat Sensors based on Pseudo-invariant Target Sites in Western Queensland, Australia", In Proceedings of IEEE International Geoscience and Remote Sensing Symposium, Vol. 6, pp. 3729 - 3732 Anchorage, AK.

Vriesa, D., Danahera, Denhama, Scartha & Phinnb. 2007, "An operational radiometric calibration procedure for the Landsat sensors based on pseudo-invariant target sites", Journal of Remote Sensing of Environment, Vol. 107, No. 3, 12, pp. 414-429.

Wang, T., Brosius, J.W. Thomas, R.J., Rabin, D.M. & Davila, J.M. 2009, "Absolute Radiometric Calibration of The Eunis-06 170−205 A Channel and Calibration Update for CDS/NIS", Astrophysical Journal Supplement, Vol. 86, pp. 222-232.